J Mol Model (2011) 17:1007–1016
DOI 10.1007/s00894-010-0801-x

ORIGINAL PAPER

Search for structures, potential energy surfaces, and stabilities of planar B_nP(n=1~7)

Rongwei Shi · Jingling Shao · Cheng Wang · Xiaolei Zhu · Xiaohua Lu

Received: 6 January 2010 / Accepted: 6 July 2010 / Published online: 21 July 2010

Abstract We have systematically explored and investigated the geometrical structures, stability, growth pattern, bonding character, and potential energy surface (PES) of the possible isomers of each cluster for planar B_nP (n=1~7) at the CCSD (T)/6-311+;G(d)//B3LYP/6-311+G(d) level. A large number of planar structures for the possible isomers of B_nP (n=1~7) and transition states are located. Isomers **1a~7a** of B_nP are the lowest-energy structures and **2a, 4a**, as well as **6a** are more stable than their neighbors. For the lowest-energy structures (**1a~7a**) of B_nP, P atom lies at the apex and tends to form two B-P bonds with boron atoms. They exhibit planar zigzag growth feature or approximately spherical-like growth pattern. Results from molecular orbital analysis demonstrate that the formation of the delocalized π MOs and the σ-radial and σ-tangential MOs plays a critical role in stabilizing the structures of lowest-energy isomers (**2a~7a**) of B_nP. Importantly, isomers **3a, 3c, 3d, 4a, 4b, 5b,** and **5c** of B_nP are stable both thermodynamically and kinetically at the CCSD(T)/6-311+G(d)// B3LYP/6-311+G(d) level and detectable in laboratory, which is valuable for further experimental studies of B_nP.

Keywords Cluster · DFT · Isomerization · Potential energy surfaces (PES) · Stability

Electronic supplementary material The online version of this article (doi:10.1007/s00894-010-0801-x) contains supplementary material, which is available to authorized users.

R. Shi · J. Shao · C. Wang · X. Zhu (✉) · X. Lu (✉)
State Key Laboratory of Materials-Oriented Chemical Engineering,
College of Chemistry and Chemical Engineering,
Nanjing University of Technology,
Nanjing 210009, China
e-mail: xlzhu@njut.edu.cn
e-mail: xhlu@njut.edu.cn

Introduction

The geometries, electronic structures, and stability of clusters, especially for mixed III–V group clusters, have received considerable attention in theoretical and experimental studies [1–17] in recent years.

Boron clusters and doped boron clusters have attracted much interest both theoretically and experimentally [18–21], partly because of the desire of understanding how structures and physical properties evolve from atom to the bulk phase and partly because of the potential applications of cluster-based materials in different fields [22–48]. The equilibrium geometries and atomization energies for the ground states of B_2~B_4 and B_6 have been reported at the MP4/6-31G(d) level by Whiteside [47]. Boustani investigated the geometry and electronic structures of B_n (n≤14) clusters based on quantum-chemical methods [35]. Yang et al. studied the geometries, potential energy curves, and spectroscopic dissociation energies of ground and low-lying electronic states of B_2 and B_2^+ using the *ab initio* quadratic CI calculation and 6-311G basis sets [49]. The neutral and anionic structures of B_3 and B_4 have been investigated using photoelectron spectroscopy and *ab initio* calculations by Zhai et al. [24]. The structure and stability of B_n (n=5, 6, 7) have been systematically studied by Li and Ma based on the MP2 and density functional theory (DFT) methods, respectively [40, 41, 50]. B_8 clusters were investigated by Li and coworkers based on the MP2 and DFT methods [51]. Interestingly, experimental and computational studies revealed that small pure boron clusters tend to form planar or quasi-planar structures.

It is well known that BP compound is refractory semiconductor and of considerable interest in solid state physics. The investigations on the geometrical growth feature and bonding nature in small clusters of technologically important material are interesting and challenging. So far, there have been some reports about P-doped boron clusters. Linguerri et al. carried out large scale *ab initio* calculations on the photoelectron spectra, dipole moments, spectroscopic constants, infrared, and UV radioactive transition probabilities of boron monophosphide and its negative ion [52]. The geometry, harmonic vibrational frequencies, electronic structures, and stability of the isomers of $(BP)_n$ (n=2~4) clusters have been explored by Qu et al. using the DFT technique. Results demonstrated that the ground state structures of B_nP_n (n=2, 3) clusters are similar to those of their corresponding B_nN_n (n=2, 3) counterparts [53]. However, there is no report about isomeric mechanisms of B_nP. In the current work, we perform systematical research to explore the geometrical structures, stability, growth pattern, bonding character, and potential energy surface(PES) of the possible isomers for planar B_nP (n=1~7) at the CCSD(T)/6-311+G(d)// B3LYP/6-311+G(d) level. The lowest-energy structures of B_nP exhibit planar zigzag growth feature or approximately spherical-like growth pattern. Results from NBO and molecular orbital analyses reveal that the formation of the delocalized π MOs, and the σ-radial and σ-tangential MOs contributes largely for the stabilization of lowest-energy isomers (**2a~7a**) of B_nP. It is interesting to find that isomers **3a, 3c, 3d, 4a, 4b, 5b**, and **5c** of B_nP are stable both thermodynamically and kinetically at the CCSD(T)/6-311+G (d)// B3LYP/6-311+G(d) level, which is promising for their future observation in laboratory or in interstellar space.

Computational methods

Initial structures of the B_nP (n=1~7) clusters are optimized at the B3LYP [54] /6-311+G(d) level. The vibrational frequency analysis is performed at the same level to examine whether the optimized structures are stable. In order to gain insights into the relative stability of B_nP clusters, binding energy, fragmentation energy, and second-order difference of total energies are estimated. Then, in order to examine the isomerization of singlet B_3P, triplet B_3P, double B_4P, quartet B_4P, and triplet B_5P, transition states are searched at the B3LYP/6-311+G(d) level followed by energy calibration at the CCSD(T)/6-311+G(d) level. For the transition states, the intrinsic reaction coordinate (IRC) computations are carried out at the B3LYP/6-311+G(d) level to examine whether they connect the related isomers. All computations are carried out using the GAUSSIAN 09 program package [55].

Results and discussion

79 optimized structures of B_nP (n=1~7) and 23 transition states are shown in Fig. 1 and Fig. SI-1 (in the supporting information), respectively. The lowest-energy structures of B_nP (n=1~7) are **1a, 2a, 3a, 4a, 5a, 6a, 7a** also shown in Fig. 1. The relative energies of the possible isomers of B_nP (n=1~7) and transition states are listed in Tables 1 and 2, respectively, at the B3LYP/6-311+G(d) and CCSD (T)/6-311+G(d) levels. Vibrational frequency analysis in Tables SI-1 to SI-3 demonstrates that the geometries of the isomers shown in Fig. 1 and Table 1 are stable at the B3LYP/6-311+G(d) level. It is noted that the strongest IR peaks for lowest-energy isomers (**1a~7a**) of B_nP are 954, 398, 593, 1311, 1377, 1237, and 1431 cm^{-1}, respectively. The peaks with the frequency range of 1310~1450 cm^{-1} may correspond to the stretching vibrations of B-B bonds while the peak of 954 cm^{-1} may be caused by the stretching vibrations of B-P bond. The peaks in 390~600 cm^{-1} are attributed to the in-plane bending vibrations of B-B-B and B-P-B.

Equilibrium geometry, bonding character, and stability

BP and $\mathbf{B_2P}$: As shown in Fig. 1, the ground state (**1a**) of BP is a linear structure with triplet state $^3\Pi$ in $C_{\infty V}$. Another low-lying isomer (**1b**) with $^1\Sigma$ is 8.0 and 7.8 kcal·mol^{-1} higher than the ground state of BP at the CCSD(T)/6-311+G(d) and CCSD(T)/6-311++G(3df,2pd) levels, respectively, which is consistent with the results from Linguerri [52]. It is found that the lowest-energy structure (**2a**) of B_2P is the $^2A'$ state in C_s and has two B-P and one B-B bond lengths of 1.998, 1.723, and 1.525Å, respectively. The linear isomer **2b** with the $^2\Sigma$ state in $C_{\infty V}$ is 13.0 kcal·mol^{-1} higher than the ground state of B_2P. **2c** has the isosceles triangular structure (C_{2V}, $^4B_2$) with 25.4 kcal·mol^{-1} higher than **2a**. The structure of **2d** with the $^4\Sigma$ state in $C_{\infty V}$ is similar to that of **2b**. Isomer **2e** has an isosceles triangular structure (C_{2V}, $^4B_1$) with 72.1 kcal·mol^{-1} higher than **2a**, which can be obtained by lengthening the B-B bond of isomer **2c**.

$\mathbf{B_3P}$**:** The lowest-energy structure (**3a**) with the $^1A_1$ state in C_{2V} for B_3P exhibits planar rhombus structure. The isomer **3b** (C_{2V}, $^1A_1$) can be obtained by lengthening the central B-B bond of **3a**, which is energetically less favorable by 7.4 and 7.4 kcal·mol^{-1} than **3a** at the CCSD(T)/6-311+G(d) and CCSD(T)/6-311++G(3df,2pd) levels, respectively. Isomer **3c** with planar rhombus geometry is 11.9 kcal·mol^{-1} higher than **3a**. **3d** (C_{2V}, $^3B_2$) exhibits fan-like geometry. For isomer **3e-3j**, the P atom tends to bond with one B atom. Among these isomers, **3g** is a linear structure with 47.4 kcal·mol^{-1} higher than **3a**; **3e** is a bent structure which is only 3.8 kcal·mol^{-1} lower than **3g**; **3g** and **3f** are nearly isoenergetic. **3k** is also a bent isomer with higher energy.

B_4P: Twenty low-lying isomers are located for B_4P as shown in Fig. 1. The lowest-energy structure 4a with the $^2A''$ state in C_s can be derived by capping a boron atom to B-B bond at the top right corner of 3a. The geometry of 4b is similar to that of 4a and it lies 29.7 kcal·mol^{-1} above 4a. 4c~4s isomers have higher energy. It is interesting to find that

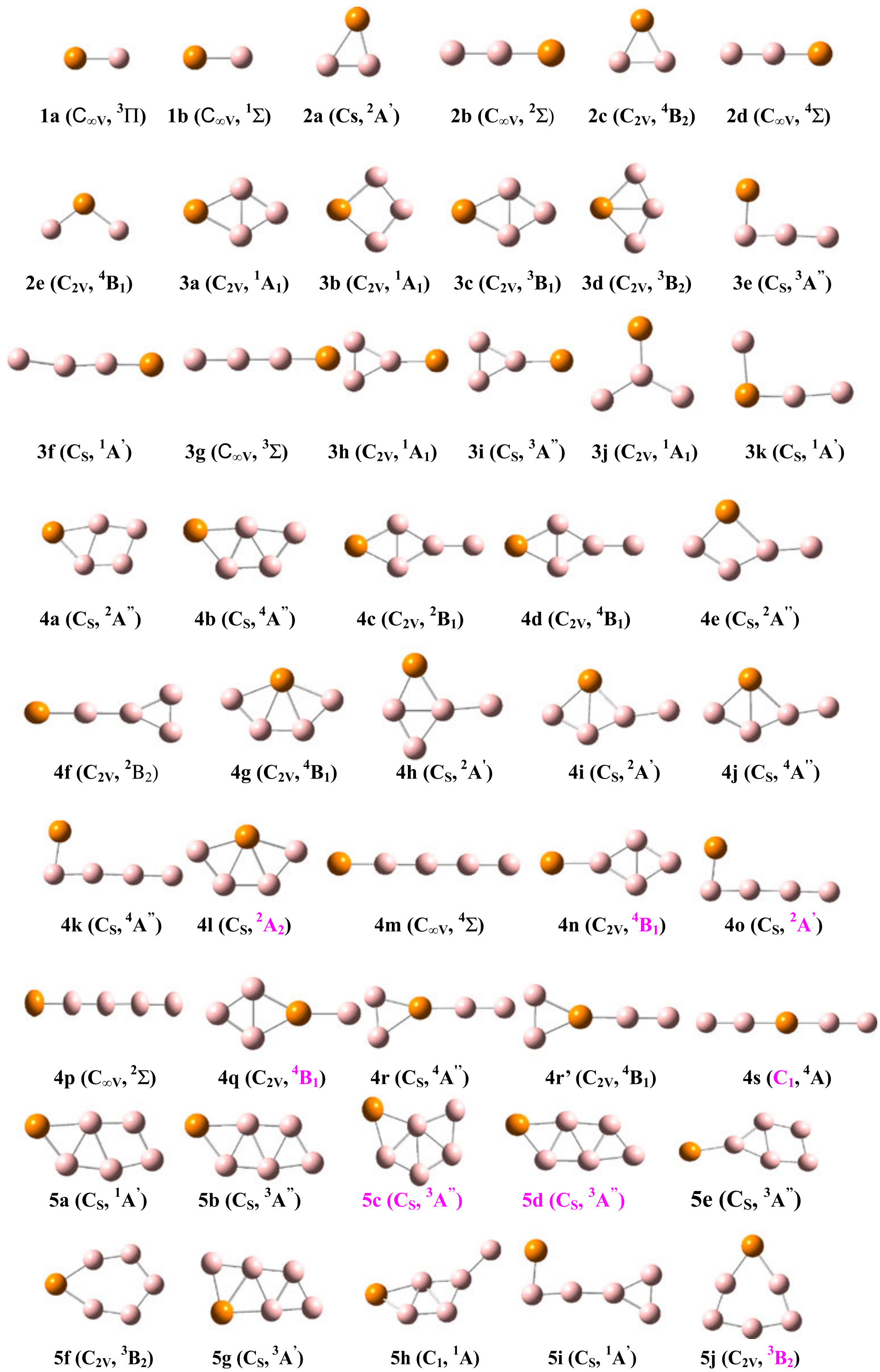

Fig. 1 Optimized geometries of the possible isomers of planar B_nP(n=1~7) at the B3LYP/6-311+G(d) level. The Arabic numbers are used to display the number of boron atoms in isomers. The point groups and electronic states are represented in parenthesis. The orange and pink bls account for phosphorus and boron atoms, respectively

there are one (for 4f, 4k, 4m, 4n, 4o, and 4p), two (for 4a~4e, 4h, and 4s), three (for 4i, 4j, 4q, 4r, and 4r'), and four B-P bonds (for 4g and 4l) between P atom and B atoms.

B_5P: In the case of B_5P, low-lying isomers are obtained as shown in Fig. 1 (they are marked as **5a~5u** in the order of energy increasing). **5a** with the $^1A'$ state in C_s can be derived through capping a boron atom to the B-B bond at the bottom right corner of **4a**. It is a planar six-membered ring containing one three-membered boron ring and one four-membered boron ring. **5b~5u** isomers have higher

Fig. 1 (continued)

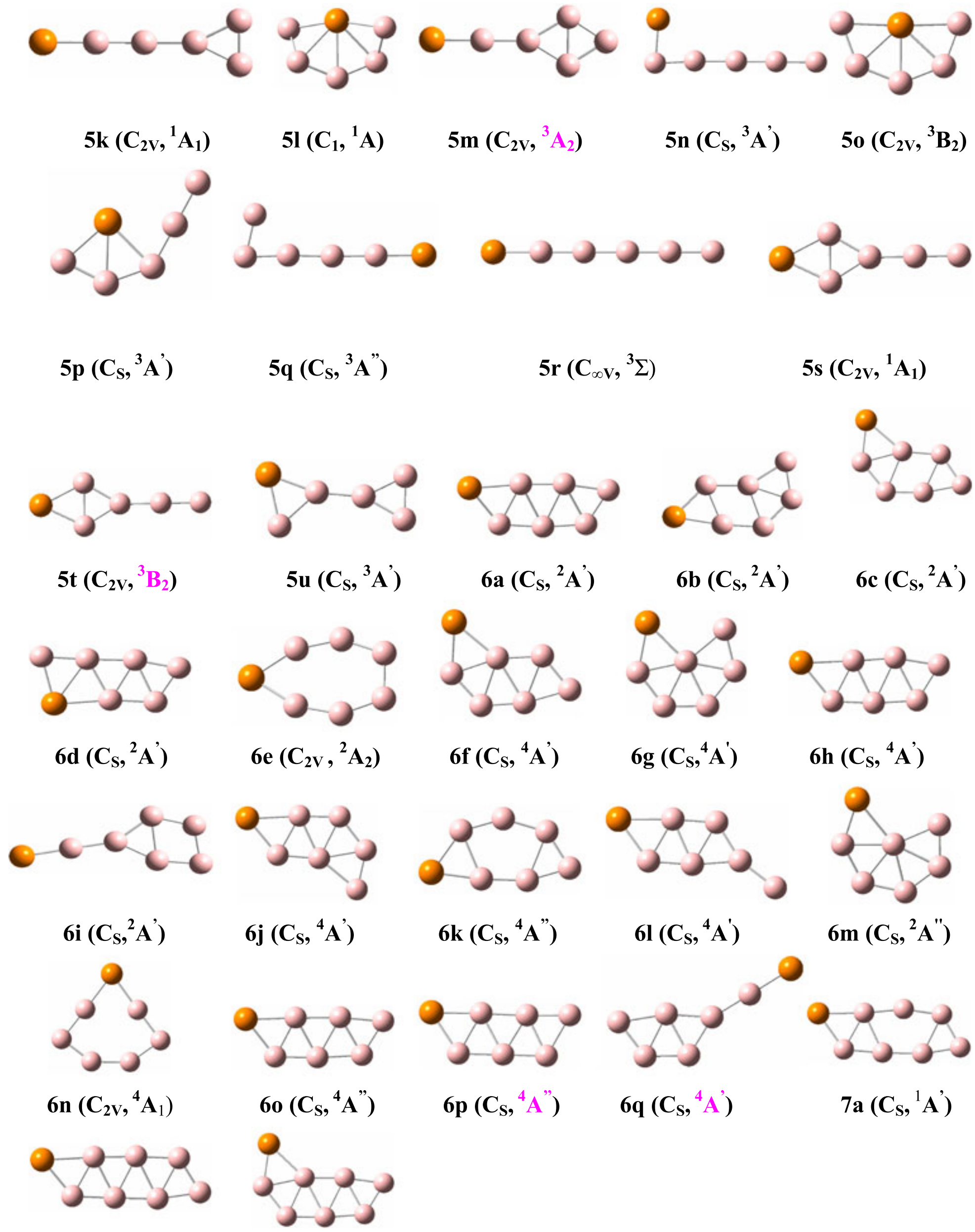

energy. It is found that there are five bonds between P and B atoms for **5l** and **5o**.

B_6P and B_7P: The lowest-energy structure **6a** with the $^2A'$ state in C_s can be obtained by capping a boron atom to B-B bond at the top right corner of **5a**. **6b** is 7.3 and 7.7 kcal·mol^{-1} higher than **6a** at the CCSD(T)/6-311+G(d) and CCSD(T)/6-311++G(3df,2pd) levels, respectively. Other isomers (**6c~6q**) have higher energy. For B_7P, three isomers are located. **7a** can be generated by capping a boron atom to B-B bond at the bottom right corner of **6a**. **7b** and **7c** are 14.8 and 19.7 kcal·mol^{-1} higher that of **7a,** respectively. Locating other possible isomers of B_7P is in progress.

It is interesting to note from the above discussion that the lowest-energy structures of B_nP (n=1~7) exhibit zigzag planar growth pattern, or approximately spherical-like pattern. As demonstrated in Fig. 2, the binding energies per atom for the lowest-energy structures B_nP (n=1~7) decrease with $N^{-1/3}$ (N=n+1), suggesting the spherical-like cluster growth pattern [56].

The relative stability of clusters can be predicted by estimating the average binding energy and fragmentation energy. The average binding energy per atom for B_nP can be defined by the following formula: $E_b(n)$ = [nE(B)+E(P)-E (B_nP)]/(n+1), where E(B), E(P), and E(B_nP) represent the

Table 1 Relative energies ($kcal mol^{-1}$) of low-energy isomers of B_nP (n=1-7) at the B3LYP/6-311+G(d) and CCSD(T)/6-311+G(d) levels

Cluster	Isomer	ΔE_1[a]	ΔE_2[b]	Cluster	Isomer	ΔE_1[a]	ΔE_2[b]	Cluster	Isomer	ΔE_1[a]	ΔE_2[b]	Cluster	Isomer	ΔE_1[a]	ΔE_2[b]	Cluster	Isomer	ΔE_1[a]	ΔE_2[b]
BP	1a[c]	0.0	0.0		3k	71.4	69.4		4q	111.2	120.0		5n	75.8	84.4		6j	52.3	52.8
	1b[c]	16.2	8.0	B_4P	4a	0.0	0.0		4r	118.1	121.5		5o	82.7	84.4		6 k	60.4	54.2
B_2P	2a	0.0	0.0		4b	26.8	29.7		4r'	116.8	125.2		5p	85.2	90.4		6 l	52.5	54.3
	2b	10.7	13.0		4c	53.3	39.4		4s	121.3	131.9		5q	78.5	91.6		6 m	29.0	57.2
	2c	26.3	25.4		4d	36.9	41.2	B_5P	5a	0.0	0.0		5r	77.5	94.4		6n	56.6	62.3
	2d	44.4	50.7		4e	76.6	50.0		5b	9.3	12.5		5 s	90.9	97.5		6o	61.2	63.7
	2e	69.9	72.7		4f	55.4	54.3		5c	22.6	19.5		5t	68.8	111.2		6p	48.5	76.6
B_3P	3a[c]	0.0	0.0		4g	53.7	54.7		5d	16.9	20.4		5u	82.4	111.5		6q	71.4	94.7
	3b[c]	12.8	7.4		4h	57.4	54.8		5e	35.8	40.7	B_6P	6 a[c]	0.0	0.0	B_7P	7a	0.0	0.0
	3c	6.4	11.9		4i	58.3	56.8		5f	37.3	43.3		6b[c]	8.8	7.3		7b	9.5	14.8
	3d	18.0	24.5		4j	54.0	57.4		5g	47.8	50.0		6c	12.0	12.4		7c	14.8	19.7
	3e	34.9	43.6		4k	53.8	57.7		5h	52.0	50.1		6d	42.2	38.1				
	3f	44.4	47.3		4l	79.8	61.1		5i	61.8	55.3		6e	38.8	42.4				
	3g	34.2	47.4		4m	53.0	67.1		5j	63.5	60.8		6f	43.1	44.6				
	3h	49.6	48.5		4n	46.8	68.7		5k	67.3	65.8		6 g	45.7	45.1				
	3i	37.7	55.1		4o	62.3	106.5		5l	82.7	73.9		6 h	43.8	45.7				
	3j	65.9	63.4		4p	61.5	116.1		5m	51.5	75.2		6i	43.3	49.7				

[a] **ΔE_1** represents the relative energy at the B3LYP/6-311+G(d) level with zero point energy correction

[b] **ΔE_2** represents the relative energy at the CCSD(T)/6-311+G(d) level

[c] Isomer **1a, 3a ,and 6a** are 7.8, 7.4 and 7.7 $kcal mol^{-1}$ lower in energy than isomer **1b,3b,** and **6b** at the CCSD(T)/ 6-311++G (3df,2pd) level, respectively

total energies of the most stable B atom, P atom, and B_nP cluster, respectively. It can be seen from Fig. 3a that the binding energy gradually increases with n, that is, the stability of clusters increases during clusters grow up. The fragmentation energy can be estimated based on the following formula: E_F (n) = E($B_{n-1}P$)+E(B) − E(B_nP), where E(B), E ($B_{n-1}P$), and E(B_nP) represent the total energies of the most stable B atom, $B_{n-1}P$, and B_nP clusters, respectively. The size dependence of the fragmentation energy is shown in Fig. 3b. As shown in Fig. 3b, the local maxima of E_F (n) appear at n= 2, 4, and 6, which implies that B_2P, B_4P, and B_6P clusters are more stable than their neighbors. In cluster physics, the second-order difference of total energy, Δ_2E (n) = E (n+1)+E (n-1)-2E (n) is a sensitive quantity that reflects the relative

Table 2 Relative energies ($kcal mol^{-1}$) of transition states of B_3P, B_4P, and B_5P at the B3LYP/6-311+G(d) and CCSD (T)/ 6-311+G(d) levels[a]

Cluster	isomer	B3LYP[b]	CCSD(T)	Cluster	isomer	B3LYP[b]	CCSD(T)
B_3P(s[c])	TS3b/3a	13.5	13.3		TS4i/4o	75.7	78.2
	TS3f/3b	44.8	47.5		TS4c/4o	78.8	84.6
	TS3a/3h	50.4	47.8		TS4p/4o	66.4	115.5
	TS3j/3b	75.7	50.5	B_4P(q[c])	TS4b/4d	36.9	41.3
	TS3h/3f	53.3	51.4		TS4b/4n	49.8	57.9
	TS3j/3h	67.0	64.8		TS4j/4g	55.3	58.2
	TS3k/3b	71.5	70.2		TS4k/4j	59.0	64.9
	TS3k/3j	73.9	71.6		TS4s/4r	121.0	130.3
B_3P(t[c])	TS3c/3i	39.1	44.9		TS4j/4r	128.2	131.3
	TS3c/3d	37.1	45.5	B_5P(t[c])	TS5b/5d	31.2	36.0
	TS3g/3e	38.3	49.6		TS5b/5e	42.0	48.5
	TS3c/3e	43.9	53.1		TS5d/5g	49.7	54.8
B_4P(d[c])	TS4a/4c	40.7	47.8		TS5e/5m	57.5	69.7
	TS4i/4l	63.2	61.3		TS5b/5t	67.7	76.6
	TS4a/4i	65.7	63.7		TS5g/5o	85.6	86.9
	TS4h/4i	71.3	72.3		TS5n/5p	85.0	95.5
	TS4a/4h	57.2	77.7				

[a] The relative energies at the different levels displayed are referenced isomers 3a, 3b, 4a, 4b and 5b.

[b] The zero-point vibrational energy is included.

[c] The letters s, t, d and q represent singlet, triplet, doublet, and quartet states.

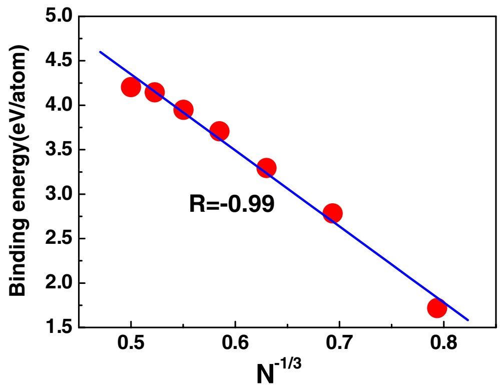

Fig. 2 The binding energy per atom vs $N^{-1/3}$ for lowest-energy isomers of B_nP (n=1~7)

stability of clusters [57]. Here E (n+1), E (n-1), and E (n) represtent the total energies of $B_{n+1}P$, $B_{n-1}P$ and B_nP clusters, respectively. Figure 3c shows the second-order difference of total energy, $\Delta_2E(n)$, as a function of n. The peaks at n=2, 4, and 6 suggest that these clusters possess relatively higher stability, which is consistent with the results obtained from Fig. 3b.

Figure SI-2 in supporting information represents some occupied molecular orbitals for **1a~7a** isomers of B_nP (n=1~7). As shown in Fig. SI-2, MO 7 of **1a** is σ molecular orbital while MO 9 and MO 11 are Π molecular orbitals. In order to examine the bonding nature for the lowest-energy isomers of B_nP, NBO analysis is performed. The Wiberg bond index (WBI) [58] of B-P bond for isomer **1a** is 2.02. For **5a**, the average WBI of bonds between circumjacent boron and phosphorus atoms is 1.30, illustrating that there is a delocalized Π bond in isomer **5a**, which is in agreement with MO 17 of isomer **5a** in Fig. SI-2. In addition, there exist σ-radial MO15 and σ-tangential MO14 for **3a** [18, 59]. It is worth noting from Fig. SI-2 that for **2a~7a**, the delocalized π MOs(MO11 of **2a**, Mo13 of **3a**, Mo18 and MO17 of **4a**, MO20 and MO17 of **5a**, MO22 and MO18 of **6a**, MO24 and MO20 of **7a**), σ-radial MOs (MO15 of **3a** and MO17 of **4a**), σ-tangential MOs(MO13 of **2a** and MO14 of **3a**) play important roles in formation of isomers **2a~7a** of B_nP.

Mulliken population analysis demonstrates that there is significant charge transfer between P and B atoms, and charge always transfers from P atom to B atoms, which may be attributed to their geometrical and electronic structures. Figure 4 reveals that the charge on P atom increases with n increasing. The positive charge on P atom increases more rapidly for n=1~4 compared to that for n=5~7. Clearly, the electronegativities (2.04 for B and 2.19 for P) of B and P atoms are close. Although the positive charge on P in **7a** is relatively larger (~0.7e), this charge transfers from P to several B atoms. Therefore, B-P bond still have the character of covalent bond in **7a**.

Isomerization and stability

The structural details of the located 23 transition states are ignored for simplicity. For the singlet isomers of B_3P, six transition states are located and their structures are shown in Fig. SI-1 and Fig. 5. Since the kinetic stability of an isomer is controlled by the smallest barrier energy, the isomer **3a** is important due to its relatively higher conversion barrier (13.3 kcal·mol^{-1} for **3a→3b)** as shown in Fig. 5. Meanwhile, its inversed barrier (**3b→3a**) is 5.9 kcalmol^{-1}, which is why 3a is more favored in kinetic stability than 3b. In addition, 3f and 3k are less stable due to their smaller inversed conversion barriers (0.2 for **3f→3b** and 0.8 kcal·mol^{-1} for **3 k→3b** at the CCSD(T)/6-311+G(d)

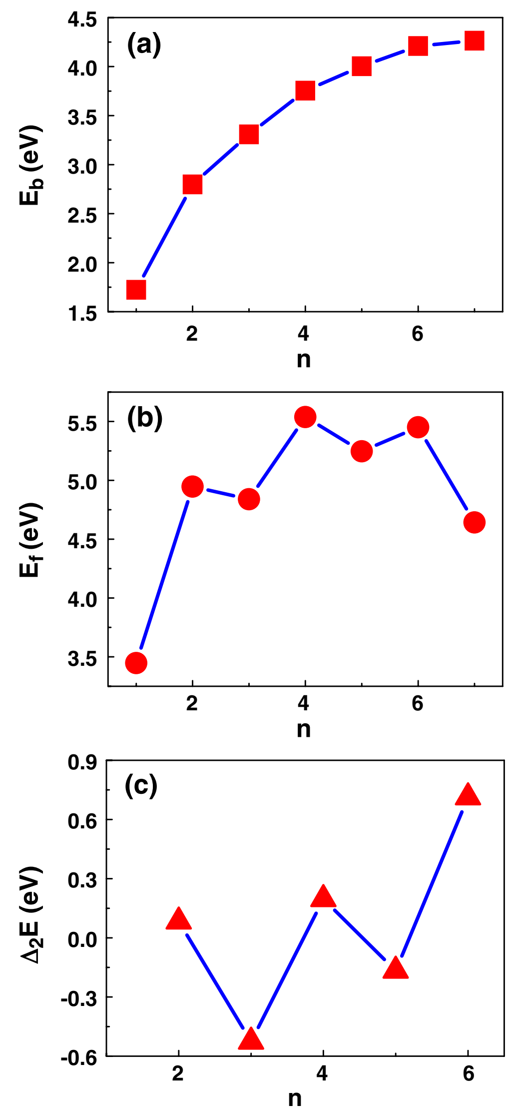

Fig. 3 The binding energy per atom (**a**), fragmentation energy (**b**), and second-order difference of total energy (**c**) versus n for the lowest-energy structures of B_nP

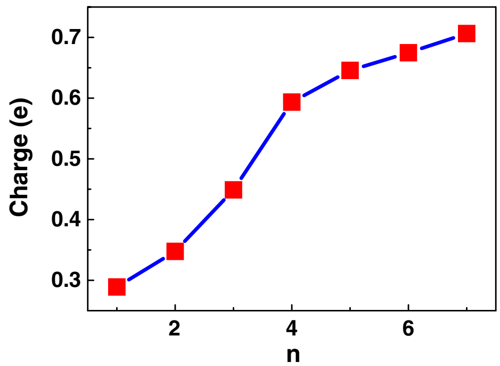

Fig. 4 Size dependence of atomic charge on P atom for the lowest-energy structures of B_nP

level) as shown in Fig. 5. It is not difficult to note from Fig. 6 that isomers **3c** and **3d** have relatively higher kinetic stability since the conversion barriers are 33.0 (**3c**→**3i**) and 21.0 kcal·mol^{-1} (**3d**→**3c**), respectively. Isomers **3e, 3g**, and **3i** have the lower kinetic stability compared with isomers **3c** and **3d**. Isomer **3g** needs smaller isomerization energy (2.2 kcal·mol^{-1}) to transfer into isomer **3e**. Isomer **3e** can be converted into isomers **3c** and **3g** through two isomerization channels with the energy barriers of 9.5 and 6.0 kcal·mol^{-1}, respectively.

In the case of doublet B_4P, five transition states are obtained. As shown in Fig. 7, from the isomerization processes described on the PES, some isomers can easily be converted to the stable isomers via overcoming small energy

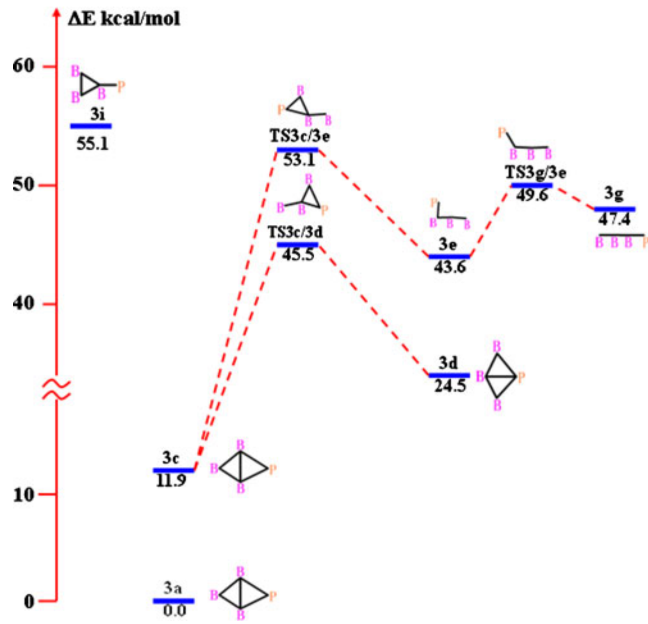

Fig. 6 Schematic potential energy surface of triplet B_3P at the CCSD(T)/6-311+G(d)//B3LYP/6-311+G(d) level

barriers. These isomers are expected to have little importance in the experimental research. The lowest-energy isomer **4a** and the high-lying species **4h** are interesting since their isomerization barriers (47.8, 22.9, and 17.5 kcal·mol^{-1} for

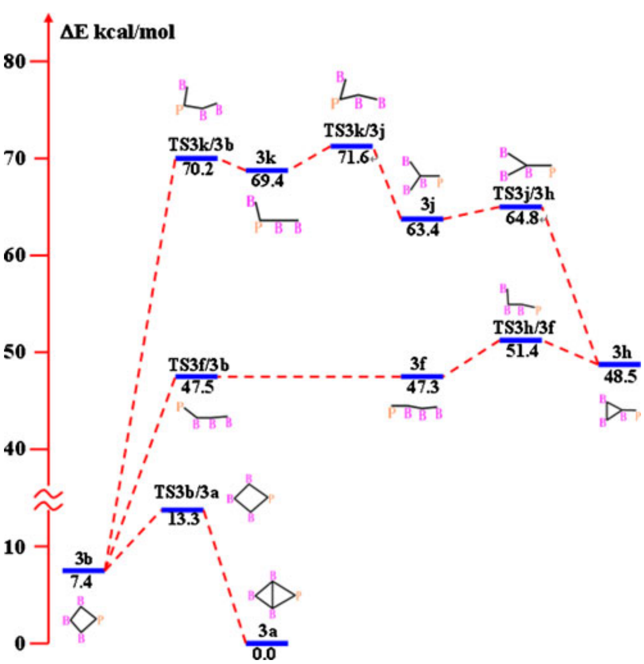

Fig. 5 Schematic potential energy surface of singlet B_3P at the CCSD(T)/6-311+G(d)//B3LYP/6-311+G(d) level

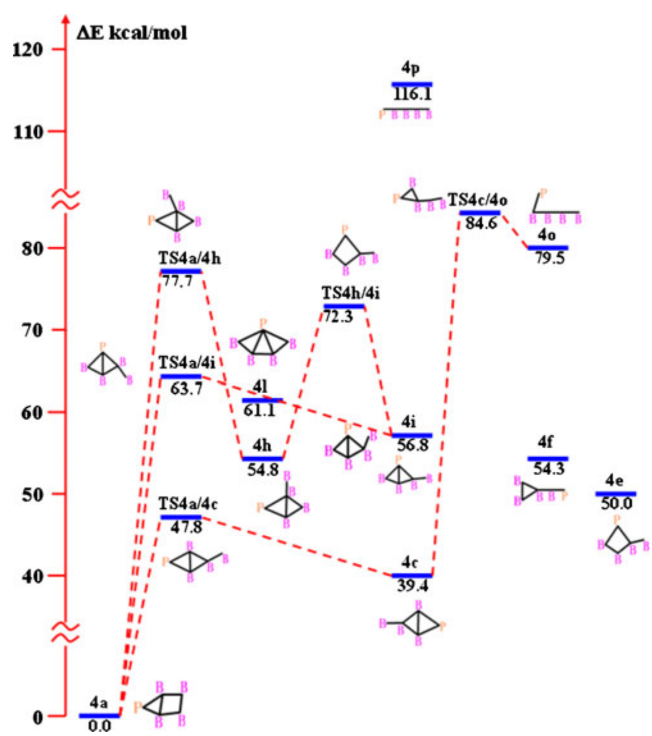

Fig. 7 Schematic potential energy surface of doublet B_4P at the CCSD(T)/6-311+G(d)//B3LYP/6-311+G(d) level

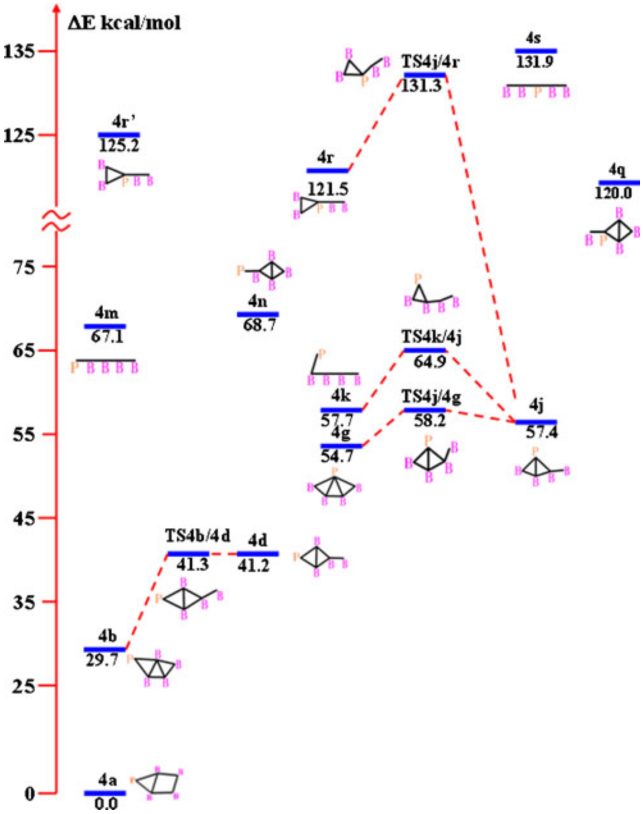

Fig. 8 Schematic potential energy surface of quartet B_4P at the CCSD (T)/6-311+G (d)//B3LYP/6-311+G(d) level

4a→4c 4h→4a and **4h→4i**, respectively) are relatively higher. **4a** with lower energy and higher conversion barrier can exist in experiment and the interstellar space. The remaining doublet isomers have much lower kinetic stability because of their higher energy or small conversion barriers. As represented in Fig. 7, the least energy barrier is 8.4 kcal·mol^{-1} (**4c→4a**). For quartet B_4P, four transition states are located as shown in Fig. 8. It is noted that only isomer **4b** is of interest with considerable kinetic stability on the PES and its isomerization barrier is 11.6 kcal·mol^{-1} (**4b→4d**). The remaining isomers are less stable due to their small conversion barriers. As shown in Fig. 8, at the CCSD(T)/6-311+G(d)// B3LYP/6-311+G(d) level, the lowest isomerization barriers of isomers **4b, 4d, 4g, 4j, 4k** and **4r** are 0.1 (**4d→4b**), 3.5 (**4g→4j**), 0.8 (**4j→4g**), 7.2 (**4k→4j**), and 9.8 kcal·mol^{-1} (**4r→4j**), respectively.

Figure 9 presents the PES of triplet B_5P. As shown in Fig. 9, two low-lying isomers **5b** and **5d** are of interest with considerable kinetic stability and they have higher kinetic stability (23.5 (**5b→5d**), 15.6 (**5d→5b**),and 34.4 kcal·mol^{-1} (**5d→5g**)). The remaining triplet B_5P are kinetically unstable. The smaller isomerization barriers are 7.8 (**5e→5b**), 4.8 (**5g→5d**), 2.5 (**5o→5g**), 11.1 (**5n→5p**) and 5.1 kcal·mol^{-1} (**5p→5n**), respectively.

Comparison with pure boron clusters and some boron-rich clusters

According to the lowest-energy structures of B_nP (n=1~7) shown in Fig. 1, it is interesting that these structures are very similar to pure boron clusters obtained from previous studies [24, 27, 29, 34, 40, 41]. Some of the lowest-energy structures of B_nP (n=1~7) can be obtained through replacing one boron atom of pure boron clusters using P atom. For example, the structures of isomers **1a, 2a, 3a, 4a** and **5a** are similar to those of pure boron clusters (a, b, c, e, g in Fig. 1) calculated using periodic DFT Program by Drummond et al. [60]. Isomer **2a, 3a**, and **4a** can be obtained by replacing one terminal B atom of B_3, B_4 and B_5 clusters [34] using P atom. Isomer **5a** can form from the XIII structure [28] located at B3LYP/6-311+g(d) level by replacing one terminal B atom using P atom. For the lowest-energy structures (**1a~7a**) of planar B_nP, P atom lies at the apex and P atom tends to form two B-P bonds with boron atoms, which are similar to the lowest-energy structures B_nC clusters [61]. Feng et al. [22] have performed research about

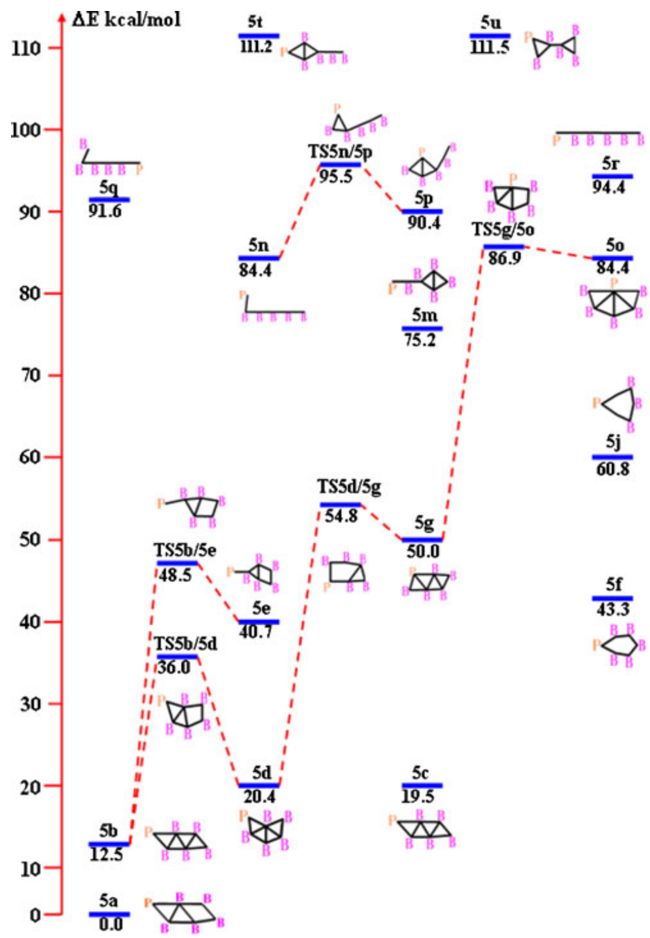

Fig. 9 Schematic potential energy surface of triplet B_5P at the CCSD (T)/6-311+G(d)//B3LYP/6-311+G(d) level

Al-doped boron clusters. They obtained some three-dimensional structures. Interestingly, the structure of isomer **3a** for B_nP is close to that of the third low-energy isomer of AlB_3 [22] with planar rhombic structure. Yang et al. [23] have studied the structures and electronic properties of FeB_n (n=1～10). They obtained a lot of geometries and these clusters tend to form three-dimensional geometries. Among these geometries, **4b, 5d** and **7b** exhibit zigzag geometries and Fe atoms lie at the apexes of the structures.

Conclusions

The equilibrium geometries, stabilities, and potential energy surfaces of possible isomers of B_nP (n=1～7) clusters are theoretically investigated at the CCSD(T)/6-311+G(d)//B3LYP/6-311+G(d) level. The main contributions are as follows: (i) the lowest-energy structures (**1a～7a**) of B_nP are located. The results of the fragmentation energy and the second-order difference of total energy demonstrate that **2a, 4a,** and **6a** are more stable than their neighbors; (ii) the lowest-energy structures of B_nP (n=1～7) clusters exhibit zigzag planar growth pattern, or approximately spherical-like growth pattern. For the lowest-energy structures (**1a～7a**) of B_nP, P atom lies at the apex and P atom appears to form two B-P bonds with boron atoms, which are similar to those of the lowest-energy structures of B_nC clusters; (iii) the delocalized π MOs, σ-radial and σ-tangential MOs contribute largely for the stabilization of isomers **2a～7a** of B_nP; (iv) the seven isomers **3a, 3c, 3d, 4a, 4b, 5b,** and **5c** of B_nP are stable both thermodynamically and kinetically, which implies that these isomers are detectable in further experiment.

Acknowledgments This work is supported by grants from the National Science Foundation of China (No. 20236010, 20246002, 20376032, 20706029, and 20876073), Jiangsu Science and Technology Department of China (No. BK2008372), and Nanjing University of Technology of China (No. ZK200803).

References

1. Raghavachari K, Rohlfing CM (1992) Structures of Si_{10}. Are there conventionally bonded low-energy isomers? Chem Phys Lett 198:521–525
2. Ho KM, Shvartsburg AA, Pan B, Lu ZY, Wang CZ, Wacker JG, Fye JL, Jarrold MF (1998) Structures of medium-sized silicon clusters. Nature 392:582–585
3. Yoo S, Zeng XC, Zhu XL, Bai J (2003) Possible Lowest-Energy Geometry of Silicon Clusters Si_{21} and Si_{25}. J Am Chem Soc 125:13318–13319
4. Yoo S, Zhao JJ, Wang JL, Zeng XC (2004) Endohedral Silicon Fullerenes Si_N ($27 \le N \le 39$). J Am Chem Soc 126:13845–13849
5. Bai J, Cui LF, Wang JL, Yoo S, Li X, Jellinek J, Koehler C, Frauenheim T, Wang LS, Zeng XC (2006) Structural Evolution of Anionic Silicon Clusters Si_N ($20 \le N \le 45$). J Phys Chem A 110:908–912
6. Asmis KR, Taylor TR, Neumark DM (1999) Electronic structure of indium phosphide clusters: anion photoelectron spectroscopy of $In_xP_x^-$ and $In_{x+1}P_x^-$ (x=1–13) clusters. Chem Phys Lett 308:347–354
7. Balasubramanian K, Zhu XL (2001) Spectroscopic properties of mixed gallium arsenide tetramers:GaAs3±, GaAs3, Ga3As±, and Ga3As. J Chem Phys 115:8858–8867
8. Cao ZJ, Balasubramanian K (2007) Unusual geometries and spectroscopic properties of electronic states of In_2N_2. Chem Phys Lett 439:288–295
9. Zhu XL, Zeng XC, Lei YA, Pan B (2004) Structures and stability of medium silicon clusters. II. Ab initio molecular orbital calculations of Si12-Si20. J Chem Phys 120:8985–8995
10. Zhu XL (2003) Spectroscopic properties for Al_2As, $AlAs_2$, and their ions. THEOCHEM 638:99–105
11. Zhu XL, Zhou ZH (2004) Electronic states for Al_2As_2 and its ions. THEOCHEM 671:105–109
12. Zhu XL (2005) Spectroscopic properties of gallium arsenide tetramers: Ga_2As_2, $Ga_2As_2^+$ and $Ga_2As_2^-$. Spectrochim Acta Part A 61:2730–2736
13. Zhu XL, Zeng XC (2003) Structures and stabilities of small silicon clusters: Ab initio molecular-orbital calculations of Si7-Si11. J Chem Phys 118:3558–3570
14. Zhu XL, Lu XH, Feng X (2007) Geometries and electronic structures of metastable C_2N_4 and its ions. Spectrochim Acta Part A 67:756–761
15. Zhu XL (2007) Theoretical study of electronic structures and spectroscopic properties of Ga_3Sn, $GaSn_3$, and their ions. Spectrochim Acta Part A 66:153–162
16. Zhu XL (2007) Jahn-Teller distortion geometries and electronic structures of Ga_3Ge, $GaGe_3$, and their ions. Spectrochim Acta Part A 66:512–520
17. Zhu XL (2005) Electronic states of Ga_3Si, $GaSi_3$, and their ions. Spectrochim Acta Part A 62:596–603
18. Islas R, Heine T, Ito K, PvR S, Merino G (2007) Boron Rings Enclosing Planar Hypercoordinate Group 14 Elements. J Am Chem Soc 129:14767–14774
19. Averkiev BB, Zubarev DY, LMi W, Huang W, Wang LS, Boldyrev AI (2008) Carbon Avoids Hypercoordination in CB6−, CB62−, and C2B5− Planar Carbon-Boron Clusters. J Am Chem Soc 130:9248–9250
20. Wang LM, Huang W, Averkiev BB, Boldyrev AI, Wang LS (2007) CB_7^-: Experimental and Theoretical Evidence against Hypercoordinate Planar Carbon. Angew Chem Int Ed 46:4550–4553
21. Exner K, PvR S (2000) Planar Hexacoordinate Carbon: A Viable Possibility. Science 290:1937–1940
22. Feng XJ, Luo YH (2007) Structure and Stability of Al-Doped Boron Clusters by the Density-Functional Theory. J Phys Chem A 111:2420–2425
23. Yang Z, Xiong SJ (2008) Structures and electronic properties of small FeB_n (n=1–10) clusters. J Chem Phys 128:184310(1)–184310(8)
24. Zhai HJ, Wang LS, Alexandrova AN, Boldyrev AI, Zakrzewski VG (2003) Photoelectron Spectroscopy and ab Initio Study of B_3^- and B_4^- Anions and Their Neutrals. J Phys Chem A 107:9319–9328
25. Zhai HJ, Kiran B, Li J, Wang LS (2003) Hydrocarbon analogues of boron cluster planarity, aromaticity and antiaromaticity. Nat Mater 2:827–833
26. Zhai HJ, Alexandrova AN, Brich KA, Boldyrev AI, Wang LS (2003) Hepta- and octacoordinate boron in molecular wheels of eight- and nine-atom boron clusters: Observation and confirmation. Angew Chem Int Ed 42:6004–6008

27. Alexandrova AN, Boldyrev AI, Zhai HJ (2004) Electronic Structure, Isomerism, and Chemical Bonding in B_7^- and B_7. J Phys Chem A 108:3509–3517
28. Alexandrova AN, Boldyrev AI, Zhai HJ (2003) Structure and bonding in B_6^- and B_6: Planarity and antiaromaticity. J Phys Chem A 107:1359–1369
29. Zhai HJ, Wang LS, Alexandrova AN, Boldyrev AI (2002) Electronic structure and chemical bonding of B_5^- and B_5 by photoelectron spectroscopy and ab initio calculations. J Chem Phys 117:7917–7924
30. Boustani I (1995) A comparative study of ab initio SCF-CI and DFT. Example of small boron clusters. Chem Phys Lett 233:273–278
31. Boustani I (1995) Structure and stability of small boron clusters. A density functional theoretical study. Chem Phys Lett 240:135–140
32. Boustani I (1997) New quasi-planar surfaces of bare boron. Surf Sci 370:355–363
33. Boustani I (1994) Systematic LSD Investigation on Cationic Boron Clusters: B_n^+(n=2-14). Int J Quantum Chem 52:1081–1111
34. Boustani I (1997) Systematic ab initio investigation of bare boron clusters: Determination of the geometry and electronic structures of B_n (n=2–14). Phys Rev B 55:16426–16438
35. Boustani I (1998) Boron in ab initio calculations. Quandt A Comput Mater Sci 11:132–137
36. Boustani I, Rubio A, Alonso JA (1999) Ab initio study of B_{32} clusters: competition between spherical, quasiplanar and tubular isomers. Chem Phys Lett 311:21–28
37. Ricca A, Bauschlicher CW (1996) The structure and stability of B_n^+ clusters. Chem Phys 208:233–242
38. Ricca A, Bauschlicher CW (1997) The structure and stability of B_nH^+. clusters. J Chem Phys 106:2317–2322
39. Niu J, Rao BK, Jena P (1997) Atomic and electronic structures of neutral and charged boron and boron-rich clusters. J Chem Phys 107:132–140
40. Li QS, Jin HW (2002) Structure and Stability of B_5, B_5^+, and B_5^- Clusters. J Phys Chem A 106:7042–7047
41. Ma J, Li Z, Fan K, Zhou M (2003) Density functional theory study of the B_6, B_6^+, B_6^- and B_6^{2-} clusters. Chem Phys Lett 372:708–716
42. Hanley L, Anderson SL (1987) Production and collision-induced dissociation of small boron cluster ions. J Phys Chem 91:5161–5163
43. Hanley L, Anderson SL (1988) Oxidation of small boron cluster ions ($B_{1\text{-}13}^+$) by oxygen. J Chem Phys 89:2848–2860
44. Hintz PA, Ruatta SA, Anderson SL (1990) Interaction of boron cluster ions with water: Single collision dynamics and sequential etching. J Chem Phys 92:292–303
45. Hintz PA, Sowa MB, Ruatta SA, Anderson SL (1991) Reactions of boron cluster ions (B_n^+, n=2-24) with N_2O: NO versus NN bond activation as a function of size. J Chem Phys 94:6446–6458
46. Sowa-Resat MB, Smolanoff J, Lapiki A, Anderson SL (1997) Inter- action of small boron cluster ions with HF. J Chem Phys 106:9511–9522
47. Whiteside RA (1981) PhD thesis, Carnegie Mellon University
48. Hanley L, Whitten JL, Anderson SL (1988) Collision-Induced Dissociation and ab Initio Studies of Boron Cluster Ions: Determination of Structures and Stabilities. J Phys Chem 92:5803–5812
49. Yang CL, Zhu ZH, Wang R, Liu XY (2001) Analytical potential energy functions of the neutral and cationic B_2. THEOCHEM 548:47–52
50. Li QS, Gong LF, Gao ZM (2004) Structures and stabilities of B_7, B_7^+ and B_7^- clusters. Chem Phys Lett 390:220–227
51. Li QS, Zhao Y, Xu WG (2005) Structure and Stability of B_8 Clusters. Int J Quantum Chem 101:219–229
52. Linguerri R, Komiha N, Oswald R, Mitrushchenkov A, Rosmus P (2008) Electronic states of BP, BP^+, BP^-, B_2P_2, $B_2P_2^-$ and $B_2P_2^+$. Chem Phys 346:1–7
53. Qu YH, Ma WY, Bian XF, Tang HW, Tian WX (2006) Electronic Structure and Stability of BP Clusters: Theoretical Calculations for $(BP)_n$ (n=2-4). Int J Quantum Chem 106:960–967
54. Becke AD (1993) Density-functional thermochemistry. III. The role of exact exchange. J Chem Phys 98:5648–5652
55. Frisch MJ, Trucks GW, Schlegel HB, Scuseria GE, Robb MA, Cheeseman JR, Scalmani G, Barone V, Mennucci B, Petersson GA, Nakatsuji H, Caricato M, Li X, Hratchian HP, Izmaylov AF, Bloino J, Zheng G, Sonnenberg JL, Hada M, Ehara M, Toyota K, Fukuda R, Hasegawa J, Ishida M, Nakajima T, Honda Y, Kitao O, Nakai H, Vreven T, Montgomery JA Jr, Peralta JE, Ogliaro F, Bearpark M, Heyd JJ, Brothers E, Kudin KN, Staroverov VN, Kobayashi R, Normand J, Raghavachari K, Rendell A, Burant JC, Iyengar SS, Tomasi J, Cossi M, Rega N, Millam JM, Klene M, Knox JE, Cross JB, Bakken V, Adamo C, Jaramillo J, Gomperts R, Stratmann RE, Yazyev O, Austin AJ, Cammi R, Pomelli C, Ochterski JW, Martin RL, Morokuma K, Zakrzewski VG, Voth GA, Salvador P, Dannenberg JJ, Dapprich S, Daniels AD, Farkas O, Foresman JB Ortiz JV, Cioslowski J, Fox DJ (2009) Gaussian 09 Revision A.02. Gaussian Inc, Wallingford
56. Haberland H (1994) Cluster of Atoms and Molecules: Theory, Experiment, and Clusters of Atoms. Springer, New York
57. Wang JL, Wang GH, Zhao JJ (2001) Structure and electronic properties of Ge_n (n=2 –25) clusters from density-functional theory. J Phys Rev B 64:205411(1)–205411(5)
58. Wiberg KB (1968) Application of the pople-santry-segal CNDO method to the cyclopropylcarbinyl and cyclobutyl cation and to bicyclobutane. Tetrahedron 24:1083–1096
59. Wodrich MD, Corminboeuf C, Park SS, von Rague Schleyer P (2007) Double aromaticity in monocyclic carbon, boron, and borocarbon rings basedon magnetic criteria. Chem Eur J 13:4582–4593
60. Drummond ML, Meunier V, Sumpter BG (2007) Structure and Stability of Small Boron and Boron Oxide Clusters. J Phys Chem A 111:6539–6551
61. Wang RX, Zhang DJ, Zhu RX, Liu CB (2007) Density functional theory study of B_nC(n=1–7) clusters. THEOCHEM 817:119–123